Off-shell and multiple scattering effects in the $p+{}^2\mathrm{H}\rightarrow 2p+n$ reaction at 156 MeV

M. L'Huillier, P. Benoist-Gueutal, and J. L. Ballot
Institut de Physique Nucléaire, Division de Physique Théorique,† 91406 Orsay, France
(Received 21 April 1975)

The nucleon-deuteron breakup reaction is analyzed in the framework of a model of single and double scattering using the off-shell t-matrix elements corresponding to several realistic local two-nucleon potentials. The multiple scattering contributions are estimated through a model derived from a fixed scattering centers approximation with a simple separable two-body t matrix.

[NUCLEAR REACTIONS $^2\mathrm{H}(p,2p)n$, $E=156$ MeV. Calculated cross section single plus double scattering including exact off-shell two-nucleon t-matrix elements and integral solution in a fixed scattering centers approximation.]

I. INTRODUCTION

A large set of experimental data[1,2] is now available for the deuteron breakup reaction initiated with 156 MeV protons; this is suitable for testing the various interpretations of this three-body reaction. However, the difficulty of the numerical computations precludes, for the time being, solving the Faddeev[3] equations with a realistic N-N interaction except at low energies.[4] Therefore, one has to use a simplified model of the reaction mechanism. At intermediate energies, the main features of the cross sections can be reproduced if one assumes a free scattering of the projectile on one target nucleon, the other remaining a "spectator."[5] Because of momentum conservation, the spectator nucleon recoils with its initial momentum in the deuteron; hence, the $^2\mathrm{H}(p,2p)n$ cross section is the product of a free N-N cross section with the deuteron momentum distribution (on-shell impulse approximation). One improves this description by taking into account an enhancement by a final state interaction (FSI) between the target nucleons[6-9] or a rescattering of the projectile on the spectator nucleon.[10] Indeed, the incorporation of "double scattering" corrections evaluated with N-N on-shell scattering amplitudes and N-N wave functions which fit the N-N experimental phase shifts leads to a better agreement with the experiment. The deviation is less than 10% in the "quasifree scattering" region QFS where one of the three nucleons is observed practically at rest in the laboratory.[11,12] However, when the available energy is almost equally shared among the three nucleons, the weight of the rescattering terms increases and results become sensitive to the N-N parametrization.

This raises the question of the occurrence of multiple scattering processes of order higher than two. The iterative resolution of the Faddeev equations furnishes a multiple scattering description of the reaction. There is no assurance of a rapid convergence for this expansion, although semiclassical arguments predict that the probability of multiple collisions decreases when the energy of the projectile increases. The importance of third order terms has been tested[13,14] for the breakup reaction at a lower energy than 156 MeV and with a separable N-N interaction. Nevertheless, the comparison with experiment suggests that beyond 60 MeV it is not necessary to calculate higher order contributions. Therefore, a double scattering model might be a good approximation for the breakup mechanism at 156 MeV.

Nevertheless, the on-shell frame previously displayed must be improved for large momentum transfers, because the energy is not conserved in each N-N collision. Corrections taking in account some off-shell effects have already been estimated,[10-12] but for a precise calculation one needs to introduce proper off-shell N-N amplitudes as required by the antisymmetrized Faddeev equations.

Conversely, following the sensitivity of the results to the nature of the two-body interaction, the analysis of the three-body breakup experiments will be a tool to look for the N-N interaction off the energy shell and to select among several on-shell-equivalent interactions.

Some calculations based on this approach of the $^2\mathrm{H}(p,2p)n$ cross section up to 100 MeV with a realistic potential have been done for the single scattering terms[15] ("off-shell impulse approximation") for which only half-shell t matrices are needed. Unfortunately, the kinematical region was too close to the QFS peak to show a sensitivity to the two-body parametrization. The lack of experimental data outside the QFS region inspired two groups at Orsay to perform measurements

in kinematical regions which favors N-N scattering very far from the shell. Although the probability of such events is very small, a final state interaction condition between the projectile and one target nucleon can be used to enhance the cross section leading to a better precision.

In order to test, through the three-body problem, different N-N local potentials with soft or hard cores,[16-19] we have computed and analyzed their fully off-shell t matrix elements.[20] The off-shell differences for relative N-N momenta and energies which are the most probable through the double scattering model were found large enough with respect to the accuracy of the measurements to strengthen our hope of discriminating among the potentials. We expect a significant potential dependence at the FSI peak where the deviation from the on-shell values is maximum and in neighborhoods of minima of the cross section where variations are enhanced by the effect of interferences.

In the first part of the present work, we have calculated the first and second order terms of the iterative solution of the fully antisymmetrized Faddeev equation and studied their sensitivity to the details of the N-N realistic potentials, such as the tensor part and short distance behavior, and to the off-shell effects. Preliminary results of our calculations have been published in the experimental papers[1,2] and in Ref. 21.

However, the question of the sensitivity of the three-body problem to the off-shell contributions of the t matrix is debatable. Recently, Wallace[22] solved the Faddeev equations and was able "to describe the gross features of N-d breakup data through 156 MeV" with a very simplified two-nucleon S-wave separable interaction averaged on the elastic N-N cross section. "This success could be explained by the possibility that three-body amplitudes may not be sensitive to the details of the two-body amplitude used to calculate them." Brayshaw[23] concludes in the same way from a new method of analysis of the deuteron breakup at 14.4 MeV. "No off-shell information can be obtained... which is not already implicit in the value of the n-d doublet scattering length." On the other hand, for the same energy Kloët[4] indicated certain regions in phase space which promise to be interesting from the point of view of the cross sections sensitivity to the details of the nuclear forces.

Now, we presently claim a real sensitivity to the off-shell behavior of realistic N-N potentials through the double scattering model. It is a matter of interest to examine if this sensitivity will be preserved when are added the multiple scattering contributions. Therefore, the second part of this paper is an attempt to estimate the error due to the truncation of the Faddeev series at second order.

Taking into account the relatively slow variation of the N-N interaction at 156 MeV and its short range character, we practice a "fixed scattering centers"[24-27] type approximation (FSA), neglecting the relative motion of the two target nucleons during the collision time. Then we parametrize the N-N t matrix in a S-wave separable form, the N-N on-shell amplitude and the range parameter being chosen in order to reproduce the results of the second order model calculation with a given realistic potential. The integral equation can be solved analytically through this approximation. The convergence of the series is examined and the sensitivity to the two-body parametrization is analyzed.

The structure of this paper is as follows: in Sec. II, we formulate the single plus double scattering model. Results of the calculation with realistic local potentials are discussed in Sec. III and compared with the experiments. In Sec. IV, the summation of the multiple scattering expansion is analyzed through the FSA model. We present conclusions in Sec. V. More details on the present work can be found in L'Huillier's thesis.[28]

II. FORMALISM

A. Notation

In the numerical calculations we have used the relativistic kinematics and taken into account the proton-neutron mass difference, but in order to simplify the formulas we neglect in the following the relativistic corrections which are small at 156 MeV and set $m_p = m_n = m$ for the nucleon mass. We use the units of $\hbar = c = 1$.

We denote by $\epsilon_d = \alpha_1^2/m$ the binding energy of the deuteron, $\vec{p}_0$, E and $\vec{p}_i$, E_i, respectively, the laboratory momenta and kinetic energy of the incident nucleon 1 and nucleon i ($i = 1, 2, 3$) in the final state. We denote also by $\vec{\lambda}_0 = \frac{2}{3}\vec{p}_0$ and $\vec{\lambda}_i = \vec{p}_i - \frac{1}{3}\vec{p}_0$ the three-body center-of-mass system (c.m.3) momenta. The nine parameters $\vec{p}_i$ are related by the four energy-momentum conservation relations.

Let us define $\vec{\chi}_i = \frac{1}{2}(\vec{p}_0 + \vec{p}_i)$, $\vec{q}_i = \frac{1}{2}(\vec{p}_0 - \vec{p}_i)$, $\vec{\mu}_i = \frac{1}{2}(\vec{p}_j - \vec{p}_k)$, where (i, j, k) is a cyclic permutation of $(1, 2, 3)$. The relative energy of the $(j-k)$ pair is denoted by $\epsilon_i = \mu_i^2/m$ and the c.m.3 energy by $E = \frac{3}{4}\lambda_0^2/m - \epsilon_d = \frac{3}{4}\lambda_i^2/m + \epsilon_i$.

B. Cross section

When nucleons 1 and 2 are detected in coincidence, the differential cross section in the labora-

tory, for a nonpolarized beam, is given by:

$$\frac{d^5\sigma}{dE_1 d\Omega_1 d\Omega_2} = FJ \ , \tag{1}$$

where

$$J = \tfrac{1}{6}\,\mathrm{Tr}\,MM^+ \ , \tag{2}$$

$$F = 8\pi^4 m \frac{p_1 p_2{}^3}{p_0 |\vec{p}_2 \cdot \vec{\mu}_1|} \ . \tag{3}$$

The quantity F is a kinematical factor, whereas M is an operator on the spin space of three nucleons:

$$M = -(2)^{1/2} \langle \tau_F | N | \tau_I \rangle \Lambda_1 \ . \tag{4}$$

Λ_1 is the projection operator on the subspace of triplet states for nucleons 2 and 3 initially bound in the deuteron. $|\tau_I\rangle$ and $|\tau_F\rangle$ are the initial and final isospin states. The operator N on the spin-isospin space of three nucleons,

$$N = \langle \vec{\lambda}_1, \vec{\mu}_1 | U | \vec{\lambda}_0, \varphi_d \rangle \ , \tag{5}$$

is calculated as a matrix element of the transition operator U in the three-body center-of-mass system.

We introduce the coordinates

$$\vec{r} = \vec{r}_1 - \tfrac{1}{2}(\vec{r}_2 + \vec{r}_3), \quad \vec{\rho} = \vec{r}_2 - \vec{r}_3 \ . \tag{6}$$

The final and initial momenta $\vec{\lambda}_1$ and $\vec{\lambda}_0$ defined in Sec. II A are conjugate to $\vec{r}$ and the momentum $\vec{\mu}_1$ to $\vec{\rho}$. The plane wave normalization is $\langle \vec{r} | \vec{\lambda} \rangle = (2\pi)^{-3/2} e^{i\vec{\lambda}\cdot\vec{r}}$. The normalized target deuteron wave function is represented by

$$\langle \vec{\rho} | \varphi_d \rangle = (4\pi)^{-1/2} [u(\rho) + (8)^{-1/2} S_{23}(\vec{\rho}) w(\rho)] \ , \tag{7}$$

where $S_{23}(\vec{\rho})$ is the tensor operator.

C. Transition operator U

Starting from the Faddeev equations one can write the transition operator U for the fully antisymmetrized breakup amplitude as

$$U = P_1(P_1 + P_2 + P_3)[T_3(E) + T_1(E) G_0(E) X_3(E)] \ , \tag{8}$$

where $X_3(E)$ is solution of the integral equation

$$X_3(E) = T_3(E) + T_3(E) G_0(E) T_2(E) + T_3(E) G_0(E) T_2(E) G_0(E) X_3(E) \ , \tag{9}$$

$G_0(E)$ being the three-nucleon free Green function, P_i being the exchange operator in space, spin and isospin coordinates of pair (j, k). The three-body operators $T_i(E)$ are solutions of

$$T_i(E) = (1 - P_i)[V_i + \tfrac{1}{2} V_i G_0(E) T_i(E)] \ , \tag{10}$$

where V_i stands for the interaction between the nucleons j and k.

In momentum representation $T_i(E)$ is expressed in terms of the antisymmetrized two-body amplitude t_i analyzed in Ref. 5:

$$\langle \vec{p}_1', \vec{p}_2', \vec{p}_3' | T_i(E) | \vec{p}_1, \vec{p}_2, \vec{p}_3 \rangle = \delta(\vec{p}_j' + \vec{p}_k' - \vec{p}_j - \vec{p}_k) \delta(\vec{p}_i' - \vec{p}_i) t_i[\vec{\mu}_i', \vec{\mu}_i ; (mE - \tfrac{3}{4}\lambda_i^2)^{1/2}] \ . \tag{11}$$

The iterative solution of Eq. (9) gives the multiple scattering expansion of the transition operator U. The operator N defined in Eq. (5) may be written

$$N = S_3 + \mathfrak{D}_1 + \Pi_1\Pi_2(S_1 + \mathfrak{D}_2) + \Pi_1\Pi_3(S_2 + \mathfrak{D}_3) \ , \tag{12}$$

where Π_i is the exchange operator on spin-isospin coordinates of pair (j, k),

$$S_k \equiv \langle \vec{\lambda}_i, \vec{\mu}_i | T_3(E) | \vec{\lambda}_0, \varphi_d \rangle = t_3(\vec{\mu}_k, \vec{\chi}_k ; \mu_k) \varphi_d(p_k), \tag{13}$$

$$\mathfrak{D}_i \equiv \langle \vec{\lambda}_i, \vec{\mu}_i | T_1(E) G_0(E) X_3(E) | \vec{\lambda}_0, \varphi_d \rangle = \langle \vec{\lambda}_i, \Delta_{\vec{\mu}_i} | X_3(E) | \vec{\lambda}_0, \varphi_d \rangle \ . \tag{14}$$

The symbol $\Delta_{\vec{\mu}_i}$ is related to twice the scattering part of the 2-3 two-body stationary state $\psi^{(-)}_{\vec{\mu}_i}$:

$$\langle \Delta_{\vec{\mu}_i} | \vec{p} \rangle = \lim_{\eta \to 0+} \frac{1}{\epsilon_i - p^2/m + i\eta} t_1(\vec{\mu}_i, \vec{p}; \mu_i) \ . \tag{15}$$

III. SECOND ORDER CALCULATIONS WITH REALISTIC POTENTIALS

A. First order terms S_k

In the first order term S_k [Eq. (13), Fig. 1], the nucleon with momentum $\vec{p}_k$ is spectator. The two-body t_3 matrix is half-off-shell, the off-shell deviation being given by

$$\delta_k \equiv \frac{1}{m}(\chi_k^2 - \mu_k^2) = \frac{1}{m} p_k^2 + \epsilon_d = 2E_k + \epsilon_d \ . \tag{16}$$

The factor $\varphi_d(p_k)$ is maximum for $p_k = 0$ and decreases rapidly when p_k increases. The amplitude t_3 is more slowly varying, except in the case of final interaction (FSI) with a low energy ϵ_k. When δ_k is not too large, the FSI produces an enhancement of S_k. For $p_k \approx 0$, S_k is maximum and describes a quasifree, two-nucleon scattering (QFS), the t_3 matrix is nearly on-shell with $\epsilon_k \simeq \frac{1}{2} E_0$.

In the calculation of S_k, the off-shell t_3 amplitude and the deuteron wave function have been computed[5] from the following realistic two-nucleon potentials:

Hamada-Johnston[18] (HJ), Reid[19] (hard core RHC and soft-core RSC), Sprung-de Tourreil[17] (SSA) and Gogny-Pires-de Tourreil[16] (G1).

Experimental data[1,2] at 156 MeV are shown in Figs. 2–4 for typical QFS and FSI situations, in coplanar geometry. The angle θ_k between $\vec{p}_k$ and $\vec{p}_0$ is defined with the convention $-180° < \theta_k \leq 180°$. Curves J_1 are the sum of the three first order contributions to J[Eq. (2)] in fm^5 calculated with HJ potential. Figure 2 corresponds to $\vec{p}_1$ fixed: $E_1 = 50$ MeV, $\theta_1 = 45°$. In the upper part, the values of the energies E_i and ϵ_i are plotted as functions of θ_2. Quasifree p-p scattering occurs at $\theta_2 = -33°$ with $E_3 = 1$ MeV and final p-n interaction at $\theta_2 = -69°$ with $\epsilon_2 = 2.2$ MeV. In the lower part, the contributions of S_1, S_2, and S_3 are plotted separately. S_1 and S_2 are far off shell ($\delta_k \simeq 100$ MeV). For $E_3 < 5$ MeV, S_1 and S_2 are negligible, but for $-\theta_2 > 50°$ the three S_k terms interfere and their magnitudes reflect the value of the deuteron wave function for large momenta. The enhancement of S_2 in the FSI region is not strong enough to fit the experimental bump.

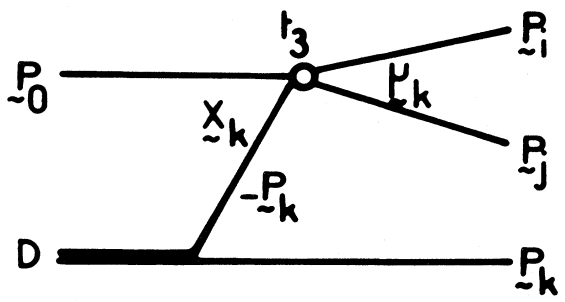

FIG. 1. Graphical representation of the amplitude S_k.

B. Second order terms D_i

The second order terms D_i correspond to the approximation $X_3(E) = T_3(E)$ in the evaluation of $\mathfrak{D}_i$ [Eqs. (9) and (14), Fig. 5]:

$$D_i = \int d\vec{p} \langle \Delta_{\vec{\mu}_i} | \vec{p} + \vec{q}_i \rangle t_3 \{ \tfrac{1}{2}(\vec{p}_0 - \vec{p}) - 2\vec{q}_i ; \tfrac{1}{2}(\vec{p}_0 - \vec{p}); [\tfrac{1}{4}(\vec{p}_0 - \vec{p})^2 - \vec{p}^2 - \alpha_1^2]^{1/2} \} \langle \vec{p} | \varphi_d \rangle . \quad (17)$$

The integral D_i has the structure of a first order amplitude for inelastic scattering: its value is nearly proportional to the form factor

$$G(\vec{\mu}_i, \vec{q}_i) \equiv \int d\vec{p} \langle \Delta_{\vec{\mu}_i} | \vec{p}_i + \vec{q}_i \rangle \langle \vec{p} | \varphi_d \rangle$$

$$= \int d\vec{p} \langle \Delta_{\vec{\mu}_i} | \vec{p} \rangle e^{-i\vec{q}_i \cdot \vec{p}} \langle \vec{p} | \varphi_d \rangle . \quad (18)$$

This function $G(\vec{\mu}_i, \vec{q}_i)$ is maximum for the smallest q_i values, especially when μ_i is small (FSI).

Though the computation of the off-shell matrix elements of t_3 allows an exact evaluation of the D_i integral, we shall use a factorization approximation to circumvent the overly long numerical calculations; we replace t_3, which varies more slowly than the other factors, by the spin-isospin operator $\langle t_3 \rangle_i$ calculated for a constant momentum:

$$\vec{p} = \vec{\nu}_i , \quad (19)$$

$$D_i = \int d\vec{p} \langle \Delta_{\vec{\mu}_i} | \vec{p} \rangle \langle t_3 \rangle_i \langle \vec{p} | \varphi_d \rangle e^{-i\vec{q}_i \cdot \vec{p}} . \quad (20)$$

The deuteron wave function being maximum for $p = 0$, we set $\nu_i = 0$. In this case

$$\langle t_3 \rangle_i = t_3[\tfrac{1}{2}\vec{p}_0 - 2\vec{q}_i , \tfrac{1}{2}\vec{p}_0; (\tfrac{1}{4}p_0^2 - \alpha_1^2)^{1/2}] \quad (21)$$

is nearly the half-shell value at a fixed energy equal to the laboratory energy E_0. The value $\nu_i = 0$ is the more justified if μ_i and q_i are small, since in that case the N-N wave function $\langle \Delta_{\vec{\mu}_i} | \vec{p} + \vec{q}_i \rangle$ is mainly a $l = 0$ state of the relative motion and is maximum for $p \simeq 0$.

In Figs. 2–4, curves J_2 give the second order contribution to function J [Eq. (2)], and curves J_{12} the first plus second order values obtained with the Hamada-Johnston potential. Figure 3 corresponds[2] to $\theta_1 = 45°$ and $\theta_2 = -57°$. At $E_1 = 69$ MeV there exists a superimposed experimental peak due to p-d elastic scattering. In the upper part the values of the energies E_i and ϵ_i are plotted as functions of E_1. Quasifree p-p scattering occurs at $E_1 = 88.2$ MeV with $E_3 = 3.35$ MeV. There are two regions of final p-n interaction, near $E_1 = 31$ MeV with $\epsilon_2 = 0.08$ MeV and near $E_1 = 110.6$ MeV with $\epsilon_1 = 0.13$ MeV. In the lower part of the figure, the contributions J_2 (i, l, T) are plotted separately with $i = 1, 2, 3$ referring to D_i, $l = 0$ and 2 to the S and D components of the deuteron wave function, respectively, and $T = 0$ or 1 to the isospin parts of $\Delta_{\vec{\mu}_i}$.

Figure 4 at $E_1 = 50$ MeV and $\theta_1 = 30°$ exhibits a final p-n interaction with energy $\epsilon_2 = 0.01$ MeV. Though this ϵ_2 value is smaller than in the previous case, J_1 has a less peaked structure because of the larger momentum transfer q_2. Figure 6 shows, as a function of ϵ_2, in the FSI region, the

experimental data and curves J_1 and J_{12} of Fig. 3. Comparing J_{12} with the curve "S" obtained by cutting the $l>0$ components in $|\Delta_{\mu_i}^{\tau}\rangle$, one notes that the $l=0$ final interaction gives the main contribution but that the neglect of $l>0$ waves indicates a nonnegligible error even at the FSI peak. The curve "C" obtained with the S deuteron wave function, shows, as it is also clear in Figs. 2–4, that one cannot neglect the D component when the momentum transfer is large. If one omits the $l>0$ waves both in initial and final states "SC" one gets fortuitously the best agreement with the experimental data.

In Fig. 6 we indicate at the FSI peak the values

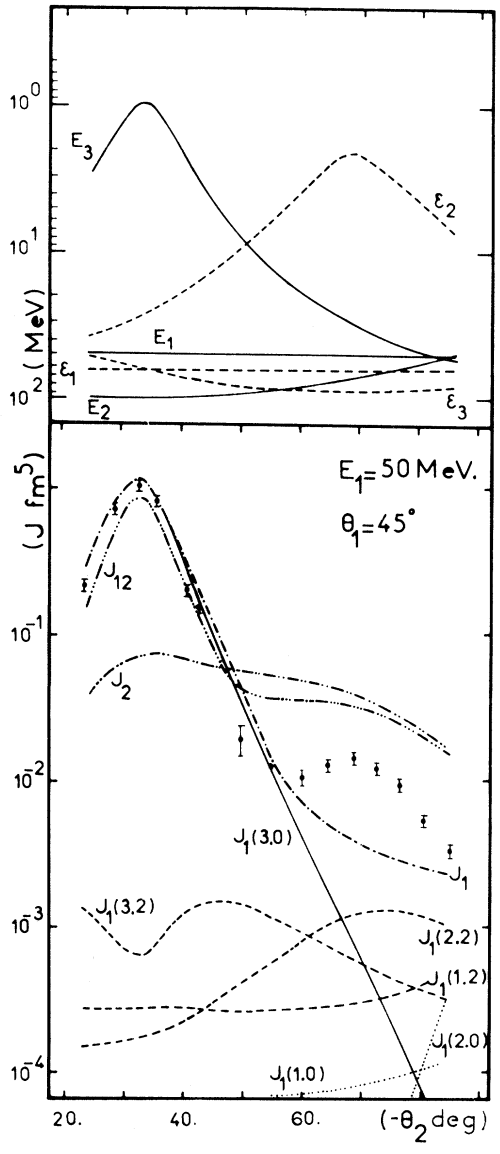

FIG. 2. ^{2}H$(p,2p)n$ reaction at 156 MeV, $E_1=50$ MeV, $\theta_1=45°$. The lower figure shows the values $J=(1/F)$ $d\sigma/dE_1 d\Omega_1 d\Omega_2$ calculated with Hamada-Johnson potential. J_1 and J_2 are the contributions of order 1 and 2 separately. J_{12} is the sum of the contributions of orders 1 and 2. The curves $J_1(k,l)$ show the contributions of amplitude S_k for the component $l=0$ or 2 of the deuteron. The experimental results are those of Ref. 1. The upper figure gives the values of E_k and ϵ_k as functions of θ_2.

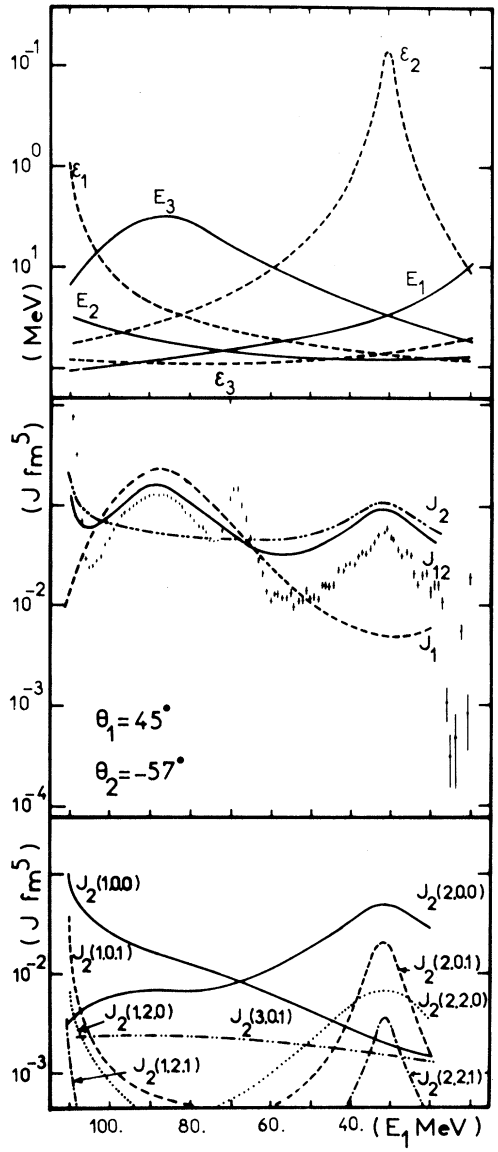

FIG. 3. ^{2}H$(p,2p)n$ reaction at 156 MeV, $\theta_1=45°$, $\theta_2=-57°$. In the lower figure, curves $J_2(i,l,T)$ show the contribution of the amplitudes D_i for the component $l=0$ or 2 of the deuteron and isospin $T=0$ or 1 of the $\Delta_{\mu_i}^{\tau}$ amplitudes. Other designations are the same as in Fig. 2. In the central figure, the experimental results are those of Ref. 2. The upper figure gives the values of E_i and ϵ_i as functions of E_1.

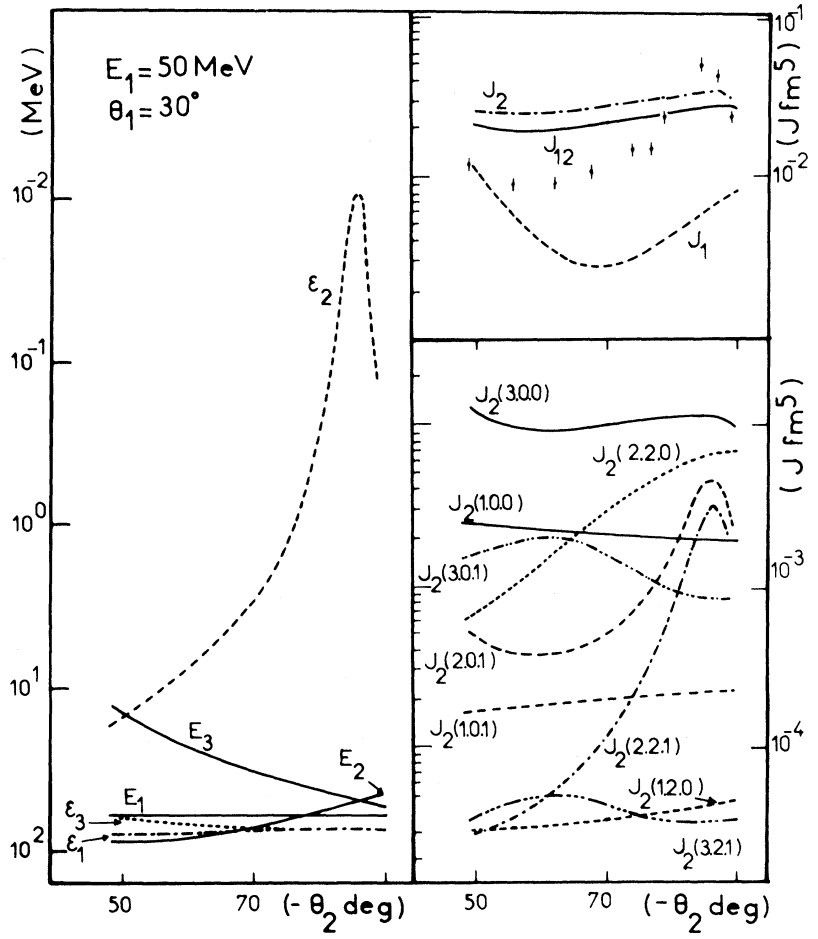

FIG. 4. ^{2}H(p,2p)n reaction at 156 MeV, $E_1 = 50$ MeV, $\theta_1 = 30°$. Designations are the same as in Fig. 3. The experimental data are those of Ref. 1.

of J_1, J_2, and J_{12} obtained with RHC (triangles), SSA (squares), and G1 (circles) potential. The spreading is about 20%. It is similar near the FSI peak in Fig. 4 but much smaller in the QFS region where the dominant first order term is nearly on shell. The differences between the potentials reveal large off-shell effects which come mainly from the second order terms, especially through the form factor $G(\vec{\mu}_i, \vec{q}_i)$ [Eq. (12)].

Let us compare the calculated values J_{12} to the experimental data.[1,2] They reproduce the structure of the experimental J but none of the potentials give a quantitative fit. In the QFS region $E_i < 5$ MeV, the first order J_1 is close to the data and J_{12} is slightly smaller than J_1. In kinematical situations intermediate between QFS and FSI, i.e., $E_i > 10$ MeV and $\epsilon_j > 2$ MeV, J_1 and J_2 are of the same order of magnitude and interfere. J_{12} is systematically larger than the data, with less deep minima. In FSI regions, $\epsilon_j < 2$ MeV, J_2 gives the main contribution and reproduces the shape of the experimental peak provided E_j is large (see Fig. 3), but J_{12} is too large. On the contrary, if E_j is small (see Fig. 4), J_{12} is less

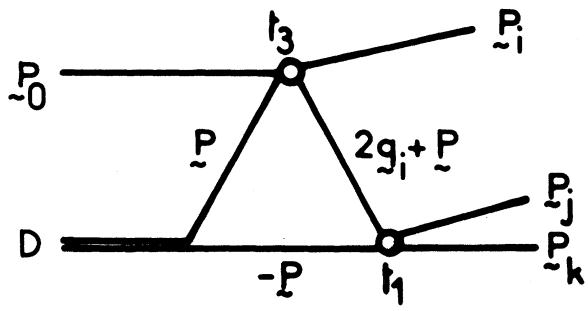

FIG. 5. Graphical representation of the amplitude D_i.

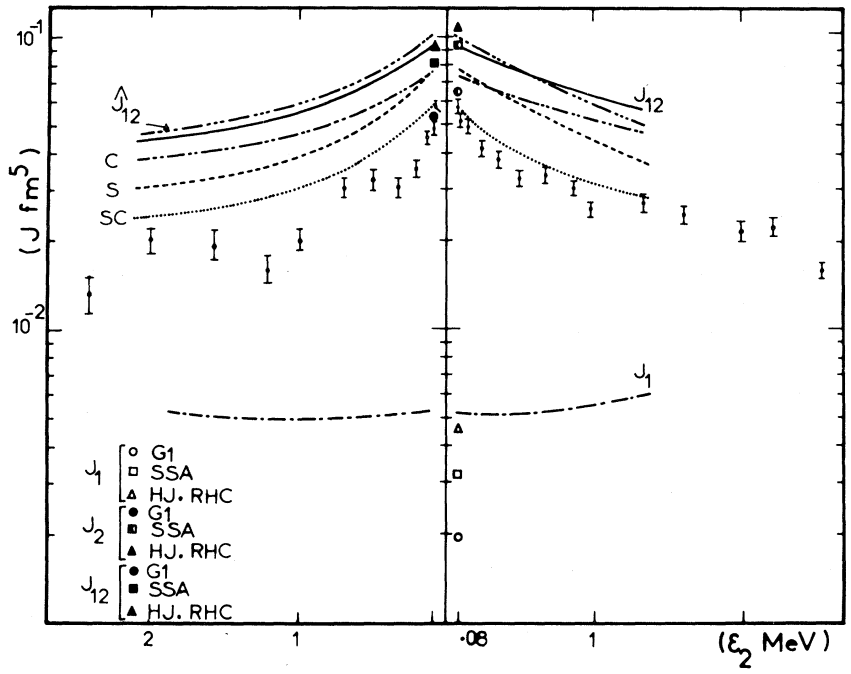

FIG. 6. $^2H(p,2p)n$ reaction at 156 MeV, $\theta_1 = 45°$, $\theta_2 = -57°$. J_1, J_2, and J_{12} have the same meaning than in the previous figures and correspond to calculations with HF potential and to the factorization with $\nu_i = 0$. J_{12} is related to a factorization with $\vec{\nu}_i = -\vec{p}_k$. Curves labeled C and S show the values of J_{12} when the D components of the deuteron and the partial wave $l > 0$ in the final state interaction are neglected, respectively. SC contains both approximations.

shaped and smaller than the experiment. Recall that, in the calculation of D_i [Eq. (18)], we made a factorization approximation. Let us remark that $\langle \Delta_{\vec{\mu}_i} | \vec{p} + \vec{q}_i \rangle$ has a pole for $|\vec{p} + \vec{q}_i| = \mu_i$; this relation is satisfied for $\vec{p} = \vec{\mu}_i - \vec{q}_i = -\vec{p}_k$. In order to test the factorization approximation with $\vec{\nu}_i = 0$ [Eq. (19)], when q_i is not small, we have tried an alternative value $\vec{\nu}_i = -\vec{p}_k$ which is to give the largest deviation from $\vec{\nu}_i = 0$ if p_k is large, i.e., μ_i or q_i is not small. In that case $\langle t_3 \rangle_i$ is the two-body t_3 matrix of the corresponding S_k term. The difference between the two calculations (curves J_{12} and $\hat{J}_{12}$ in Fig. 4) is small. The factorization cannot be held responsible for the discrepancy between the calculated and experimental values. Therefore, despite this approximation, the previous conclusions regarding the occurrence of off-shell effects remain, but the model of multiple scattering up to second order is not precise enough for discriminating among the potentials.

In order to improve the model one might try to evaluate the next multiple scattering terms. But there is no indication of a good convergence of the expansion. Besides, with realistic two-nucleon interactions one runs into increasing numerical difficulties. On the other hand, the exact solution of the Faddeev equation for energies higher than 100 MeV is, for the time being, out of computational ability. In the following section we derive a model integral equation for the N-d scattering operator based on the fixed scattering centers approximation. This model preserves the structure of the Faddeev integral equation, while avoiding the calculation of the multiple scattering expansion. We use simplified two-body interactions in order to compare with the results of the first plus second order model and to test the ability of the integral equation model to improve the fit of the experimental data.

IV. SUMMATION OF THE MULTIPLE SCATTERING SERIES IN A FIXED SCATTERER APPROXIMATION

A. Description of the model

Our model is based on the fixed scatterer approximation (FSA) used in elastic nucleon-nucleus scattering.[24,27] This approximation appears to be successful in nucleon-deuteron elastic scattering. We extend it to the breakup reaction for evaluating the terms of the multiple scattering series of orders greater than or equal to two; the first order terms S_k are supposedly exactly calculated from the off-shell N-N amplitudes.

Let us consider the $\mathfrak{D}_i$'s terms [Eq. (14)] which

describe multiple scattering process:

$$\mathfrak{D}_i = \int\int \langle \Delta_{\vec{\mu}_i} | \vec{\rho}' \rangle \langle \vec{\lambda}_i' ; \vec{\rho}' | X_3(E) | \vec{\lambda}_0 ; \vec{\rho} \rangle \langle \vec{\rho} | \varphi_d \rangle \, d\vec{\rho} \, d\vec{\rho}' . \tag{22}$$

The solution $X_3(E)$ of Eq. (9) is the elastic transition operator minus the pickup term; it implies successive scatterings of nucleon 1 on nucleon 2 and 3 initially bound in the deuteron. For small μ_i, λ_i is closed to λ_0 (FSI kinematics), the final N-N interaction of $\mathfrak{D}_i$ which is contained in the wave function $\langle \Delta_{\vec{\mu}_i} | \vec{\rho}' \rangle$ contributes mostly in the $l=0$ partial wave and its structure looks like $\langle \varphi_d | \vec{\rho}' \rangle$. Consequently, for a small final relative N-N energy ϵ_i, $\mathfrak{D}_i$ is similar to an elastic amplitude. If the FSA is valid for elastic scattering, it has to be equally valid for the evaluation of $\mathfrak{D}_i$ when $\lambda_i \simeq \lambda_0$. When μ_i is large, this approximation does not seem to be justified. But in the QFS kinematic region $p_k \simeq 0$, $\mathfrak{D}_i$ is a small correction compared to the first order S_k and can be evaluated approximately from FSA. Finally, if we calculated the three $\mathfrak{D}_i$ terms in the FSA for all kinematical regions, we hope to reproduce the maxima of the cross section and to have a good estimation of its magnitude between the peaks.

We introduce the FSA by means of two assumptions:

(i) First, the matrix elements of the free nucleon Green operator

$$\langle \vec{\lambda}' ; \vec{\rho}' | G_0(E) | \vec{\lambda} ; \vec{\rho} \rangle = \left\langle \vec{\rho}' \left| \left(E - \frac{3}{4}\frac{\lambda^2}{m} - \frac{1}{m}\Delta_{\vec{\rho}} + i\epsilon \right)^{-1} \right| \vec{\rho} \right\rangle \delta(\vec{\lambda}' - \vec{\lambda})$$

is approximated with the neglect of the binding energy ϵ_d and of the relative energy $(1/m)\Delta_{\vec{\rho}}$ corresponding to a fixed relative position of the two-target nucleons:

$$\langle \vec{\lambda}' ; \vec{\rho}' | \bar{G}_0(E) | \vec{\lambda} ; \vec{\rho} \rangle = 2M \frac{1}{\lambda_0^2 - \lambda^2 + i\epsilon} \delta(\vec{\rho} - \vec{\rho}') \delta(\vec{\lambda} - \vec{\lambda}') , \tag{23}$$

where $M = \frac{2}{3}m$ is the reduced mass in the entrance channel. With this approximation and for a local potential V without exchange one has[17]

$$\langle \vec{\lambda}' ; \vec{\rho}' | \bar{T}_{2/3}(E) | \vec{\lambda} ; \vec{\rho} \rangle = \delta(\vec{\rho} - \vec{\rho}') e^{\mp i(1/2)(\vec{\lambda} - \vec{\lambda}') \cdot \vec{\rho}} \times \langle \vec{\lambda}' | t_{2/3}(E, M) | \vec{\lambda} \rangle , \tag{24}$$

where $\langle \vec{\lambda}' | t(E, M) | \vec{\lambda} \rangle$ is the off-shell amplitude for the scattering of a particle of mass M and energy $E = \lambda_0^2/2M$ by the potential V centered at the origin.

(ii) Second, the formula (24) is supposed still valid for a local or nonlocal potential with exchange.

These two assumptions lead to a local approximation in $\vec{\rho}$ for $X_3(E)$:

$$\langle \vec{\lambda}_i ; \vec{\rho}' | \bar{X}_3(E) | \vec{\lambda}_0 ; \vec{\rho} \rangle = \delta(\vec{\rho} - \vec{\rho}') \langle \vec{\lambda}_i | Y_3(\vec{\rho}) | \vec{\lambda}_0 \rangle . \tag{25}$$

In order to get a simple analytical expression we assume for antisymmetrized two-nucleon scattering amplitudes an isotropic form:

$$\langle \vec{\lambda}' | t_i(E, M) | \vec{\lambda} \rangle = -\frac{1}{4\pi^2 M} \frac{g(\lambda, \lambda_0) g(\lambda', \lambda_0)}{g^2(\lambda_0, \lambda_0)} \times f(\lambda_0, M)(1 - \Pi_i), \tag{26}$$

with

$$g(\lambda, \lambda_0) = [\lambda^2 + \beta^2(\lambda_0)]^{-1} . \tag{27}$$

Then the solution of the integral equation (9) is given by:

$$\langle \vec{\lambda}_i | Y_3(\vec{\rho}) | \vec{\lambda}_0 \rangle = -\frac{1}{4\pi^2 M} \frac{g(\lambda_i, \lambda_0)}{g(\lambda_0, \lambda_0)} f(\lambda_0, M) e^{-(i/2)(\vec{\lambda}_0 - \vec{\lambda}_i) \cdot \vec{\rho}} [A(\vec{\rho}; \vec{\lambda}_0) - B(\vec{\rho}; \vec{\lambda}_0)\Pi_3] , \tag{28}$$

$$A(\vec{\rho}; \vec{\lambda}_0) = \frac{1 - 2x^2(\rho) + e^{-i\vec{\lambda}_0 \cdot \vec{\rho}} x(\rho)}{[1 - x^2(\rho)][1 - 4x^2(\rho)]} \tag{29}$$

$$B(\vec{\rho}; \vec{\lambda}_0) = \frac{1 + e^{-i\vec{\lambda}_0 \cdot \vec{\rho}} x(\rho)[3 - 4x^2(\rho)]}{[1 - x^2(\rho)][1 - 4x^2(\rho)]} \tag{30}$$

$$x(\rho) = -\frac{1}{2\pi^2} \frac{f(\lambda_0, M)}{g^2(\lambda_0, \lambda_0)} \int d\vec{\lambda} e^{-i\vec{\lambda} \cdot \vec{\rho}} \frac{g^2(\lambda, \lambda_0)}{\lambda_0^2 - \lambda^2 + i\epsilon} = f(\lambda_0, M) \left[\frac{e^{i\lambda_0 \rho} - e^{-\beta(\lambda_0)\rho}}{\rho} - \frac{\beta^2(\lambda_0) + \lambda_0^2}{2\beta(\lambda_0)} e^{-\beta(\lambda_0)\rho} \right] . \tag{31}$$

Finally, $\bar{\mathfrak{D}}_i$ is computed numerically from Y_3 (Eqs. 22, 25, and 28). Expansion of $\langle \vec{\lambda}_i | Y_3(\vec{\rho}) | \vec{\lambda}_0 \rangle$ in powers of $x(\rho)$, if it converges, gives a multiple scattering representation for $\bar{\mathfrak{D}}_i$. Note that the first order term obtained by setting $A = B = 1$ in Eq. (28) describes a double scattering process:

$$\bar{D}_i = \int d\vec{\rho} \langle \Delta_{\vec{\mu}_i} | \vec{\rho} \rangle \langle \vec{\lambda}_i | t_3(E, M) | \vec{\lambda}_0 \rangle e^{-i\vec{q}_i \cdot \vec{\rho}} \langle \vec{\rho} | \varphi_d \rangle \ . \tag{32}$$

It is similar to the D_i analyzed in Sec. III B for the case of the factorization approximation [Eq. (20)], the form factor is identical but the two-body interaction

$$\langle \tfrac{1}{2}\vec{p}_0 - 2\vec{q}_i | \, t_3(\tfrac{1}{2}E_0 + \epsilon_d, \tfrac{1}{2}m | \tfrac{1}{2}\vec{p}_0 \rangle$$

is now

$$\langle \tfrac{2}{3}\vec{p}_0 - 2\vec{q}_i | t_3(\tfrac{1}{3}E_0, \tfrac{2}{3}m) | \tfrac{2}{3}\vec{p}_0 \rangle \ .$$

B. Parametrization of the two-body interaction and wave functions

1. *Method for determining* $f(\lambda_0, M)$

In principle, the only parameters of the model are relative to the scattering amplitude $\langle \vec{\lambda}' | t_i(E, M) | \vec{\lambda} \rangle$ that is to say the "on-shell" value $f(\lambda_0, M) \equiv Re^{i\varphi}$ and a range parameter $\beta(\lambda_0)$. They could be fixed by fitting the off-shell scattering amplitudes for mass M, at energy E, calculated from a realistic potential. But this method applied to HJ or SSA does not give precise values for $f(\lambda_0, M)$ because the scattering amplitude is strongly anisotropic. The parameter $\beta(\lambda_0)$ which reproduces the off-shell effects is found to be increasing with the energy; for example, the results at $E_0 = 155$ MeV are compatible with values of β between 4 and 6 fm^{-1}, while at zero energy the value of β is close to 1.2–1.4 fm^{-1}.

Hence we have used an alternative method, which allows us to fix $f(\lambda_0, M)$ and to verify the self-consistency of the choice: first, we determine $f(\lambda_0, M)$ in such a way that double scattering contributions J_2 to the cross section calculated in the FSA model from the D_i's [Eq. (32)] equals the values J_2 obtained from the D_i's [Eq. (20)] with a realistic potential. As J_2 is proportional to $|f(\lambda_0, M)|^2$ this procedure gives R. Then, the phase φ can be chosen in order that J_{12} reproduce the interference between the single S_k's and double scattering amplitudes D_i's as observed in the sum J_{12}. The method works if R and φ are found independent of the kinematics.

The previous device would imply calculating the first order terms S_k's, and the wave functions $\langle \vec{\rho} | \varphi_d \rangle$ and $\langle \Delta_{\vec{\mu}_i} | \vec{\rho} \rangle$ which enter in the FSA value $\bar{J}_2$ and $\bar{J}_{12}$ from the same realistic N-N potential which provides J_1, J_2, and J_{12}. Nevertheless, our aim is to perform a qualitative analysis of the multiple scattering contributions. So, we shall substitute for the realistic wave functions and N-N interactions simpler parametrized representations which simulate the main realistic features, but remain easily manageable. Henceforth, the HJ potential will be used for reference.

2. *First order term*

Let us examine the single scattering term S_k:

$$S_k = \left\langle \vec{\mu}_k \middle| t_3\left(\frac{\mu_k^2}{m}, \frac{m}{2}\right) \middle| \vec{\chi}_k \right\rangle \varphi_d(\vec{p}_k) \ . \tag{13'}$$

(i) As the normalized Hulthén deuteron S wave function reproduces quite well the sum of the S and D density probabilities of momenta of a realistic HJ wave function, we choose for φ_d the parametrization:

$$\varphi_H(p) = \left(\frac{2}{\pi}\right)^{1/2} N_1 \left(\frac{1}{p^2 + \alpha_1^2} - \frac{1}{p^2 + \beta_H^2} \right) \tag{33}$$

with $N_1 = 0.259$ fm$^{3/2}$, $\alpha_1 = 0.232$ fm^{-1}, $\beta_H = 1.202$ fm^{-1}.

(ii) For the sake of consistency with the FSA two-body parametrization of formula (26), we adopt for the half-shell N-N scattering amplitude a separable S-wave representation in each spin channel $S = 0$ and 1:

$$\left\langle \vec{\mu} \middle| t_3^S \left(\frac{\mu^2}{m}, \frac{m}{2}\right) \middle| \vec{\chi} \right\rangle = -\frac{1}{2\pi^2 m} \frac{g_s(\chi, \mu)}{g_s(\mu, \mu)} \times \left| f_s\left(\mu, \frac{m}{2}\right) \right| e^{i\delta s(\mu)} \ , \tag{26'}$$

with form factor

$$g_s(\chi, \mu) = (\chi^2 + \beta_s^2)^{-2} \ . \tag{27'}$$

Starting from the one-rank separable potential associated with this form factor, we should obtain

$$f_s(\mu, \tfrac{1}{2}m) = \gamma_s^2 D_s^{-1}(\mu) g_s^2(\mu, \mu) \ , \tag{34}$$

with

$$\gamma_s^2 = 2\beta_s(\beta_s - (-1)^s \alpha_s)^2 \ ,$$

$$D_s(\mu) = 1 - \frac{\gamma_s^2}{2\beta_s(\beta_s - i\mu)^2} \ . \tag{35}$$

A fit of the scattering lengths and effective range parameters fixes $\alpha_0 = 0.046$ fm^{-1}, $\beta_0 \sim 1.1$–1.2 fm^{-1}, and $\beta_1 \sim 1.4$ fm^{-1}. But the N-N cross sections corresponding to amplitudes (34) are satisfying for small energies even when χ is large, but disagree with the experimental data for large μ. We then substitute in Eq. (26′) for the modulus of the elastic amplitude an average value cal-

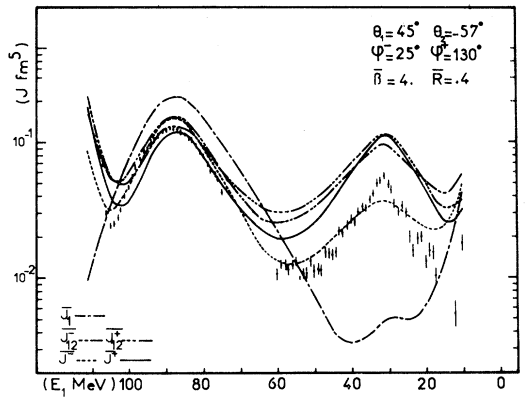

FIG. 7. ^{2}H$(p,2p)n$ reaction at 156 MeV, $\theta_1 = 45°$, $\theta_2 = -57°$ FSA cross sections $\bar{J}^{\pm}_{12}$ and the integral solutions $\bar{J}^{\pm}$.

culated from HJ potential at c.m. energy $\epsilon = (\hbar^2/m)\mu^2$ and angle $\bar{\theta}$ as follows:

$$|f_0(\mu, \tfrac{1}{2}m)|^2 = \frac{d\sigma}{d\Omega}^{T=1} \quad (\bar{\theta} = 90°) ,$$
$$|f_1(\mu, \tfrac{1}{2}m)|^2 = \frac{d\sigma}{d\Omega}^{T=0} \quad (\bar{\theta} = 60°) . \tag{36}$$

Moreover, we keep $\beta_0 = \beta_1 = \beta_H$, i.e., a value corresponding to a low energy value, because the first order terms are either on the energy shell $\mu = \chi$ (QFS), thus independent of β_s, or very small when μ and $(\chi - \mu)$ are large. We have conserved, for want of a better value, the Yamaguchi phase shift $\delta_s(\mu)$ which is suitable for small μ (FSI):

$$\delta_s(\mu) = -\operatorname{Arg} D_s(\mu) . \tag{37}$$

In fact, the corresponding first order contribution, labeled $\bar{J}_1$, is not very accurate compared to the exact J_1 whenever large interferences arise between the three S_k amplitudes [see below Figs. (7)–(10)]; so the QFS peak is slightly overestimated and $\bar{J}_1$ has too much enhancement close to the FSI kinematics at $\theta_1 = 30°$. But in the mean $\bar{J}_1$ is good enough for our proposal.

3. *Parametrization of* $\langle \Delta_{\vec{\mu}} | \vec{\rho} \rangle$

We parametrize the final N-N scattering function by a central S-wave function with a dependence on ρ corresponding to that of the deuteron and using the scattering amplitude defined through Eqs.

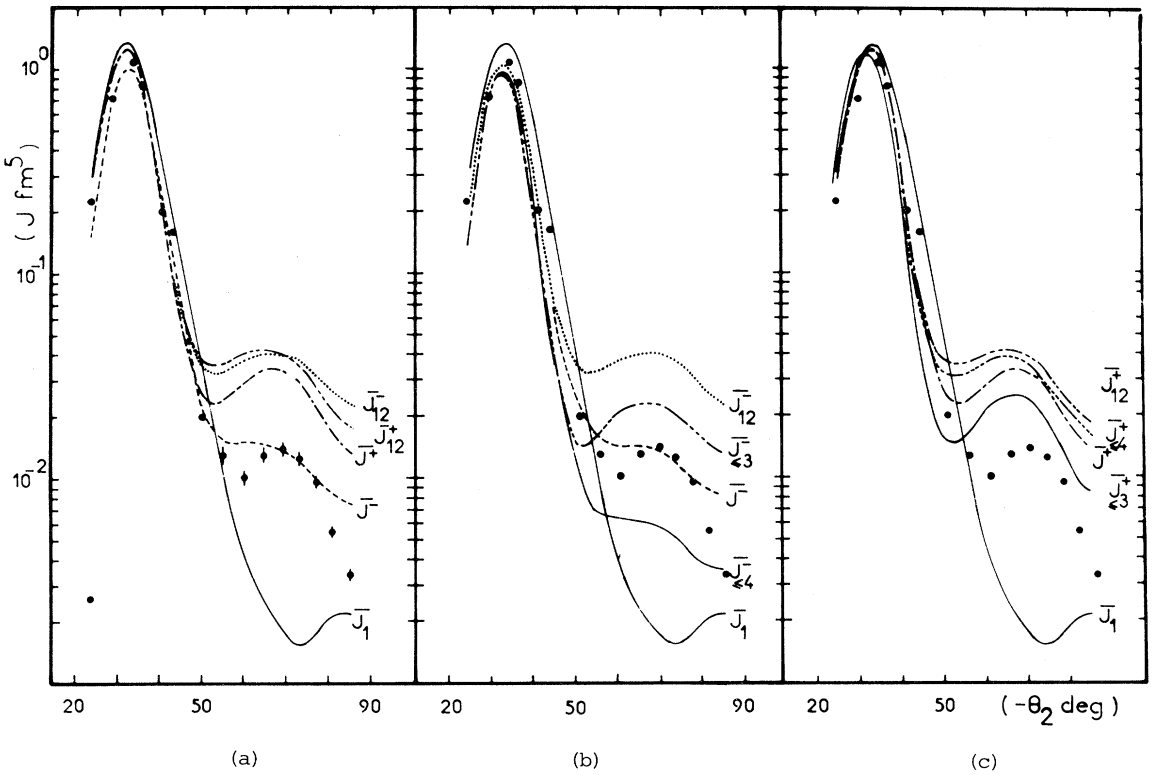

FIG. 8. ^{2}H$(p,2p)n$ reaction at 156 MeV, $E_1 = 50$ MeV, $\theta_1 = 45°$. (a) FSA cross sections $\bar{J}^{\pm}_{12}$ and the integral solutions $\bar{J}^{\pm}$. (b) FSA cross sections up to order 2, 3, and 4, calculated with $\varphi^- = 25°$. (c) FSA cross sections up to order 2, 3, and 4, calculated with $\varphi^+ = 130°$.

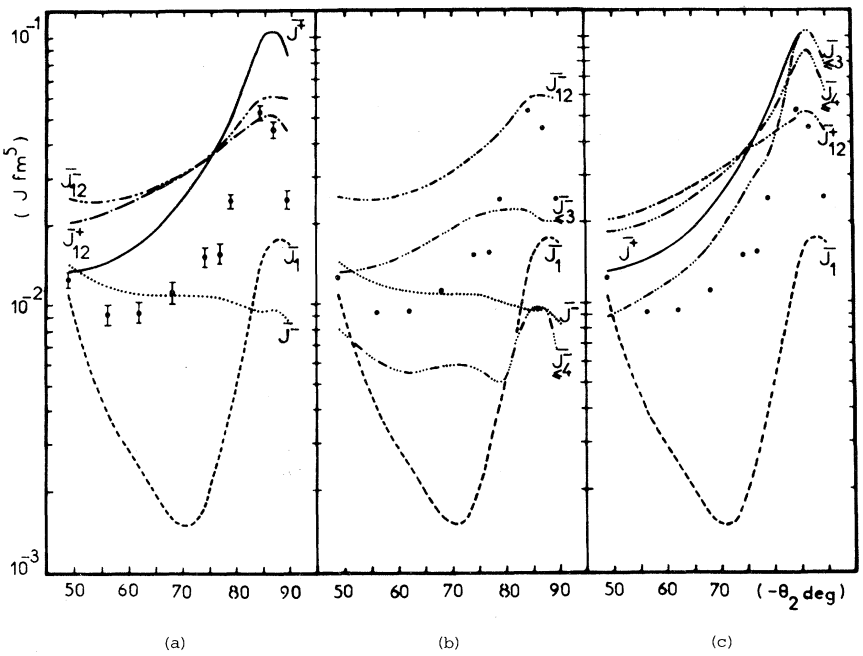

FIG. 9. $^2H(p,2p)n$ reaction at 156 MeV, $E_1 = 50$ MeV, $\theta_1 = 30°$. Designations are the same as in Fig. 8.

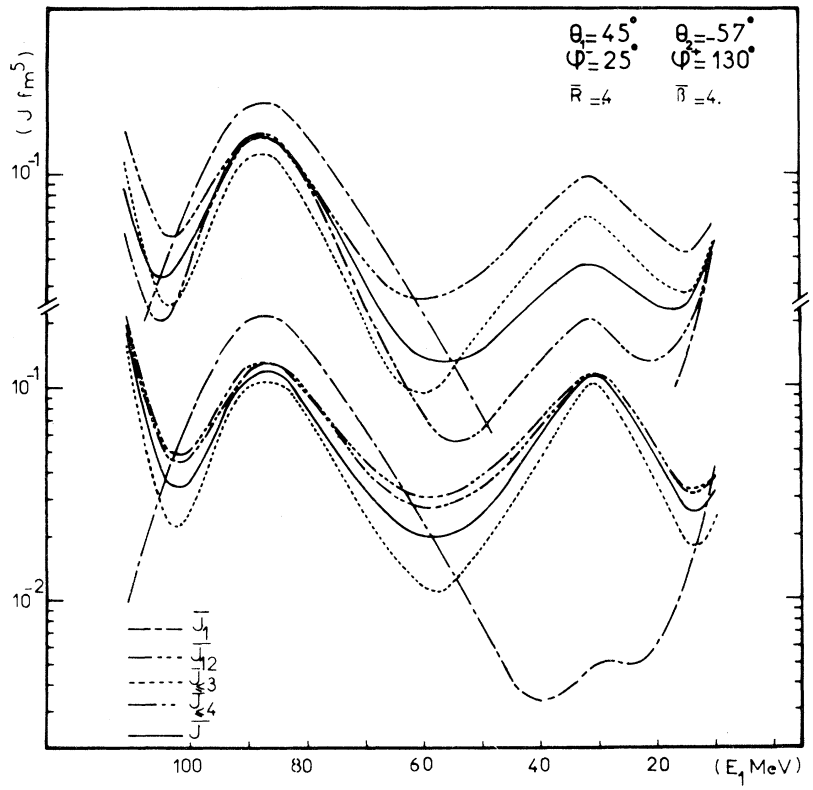

FIG. 10. $^2H(p,2p)n$ reaction at 156 MeV, $\theta_1 = 45°$, $\theta_2 = -57°$. FSA cross sections up to order 2, 3, and 4 and integral solution calculated with $\varphi^+ = 130°$ in the upper part and $\varphi^- = 25°$ in the lower part.

(26′) and (35)–(37):

$$\langle \Delta_{\vec{\mu}} | \vec{\rho} \rangle = (2\pi)^{-3/2} \frac{e^{i\mu\rho} - e^{-\beta_H \rho}}{\rho} \left\langle \vec{\mu} \left| t_1\left(\frac{\mu^2}{m}, \frac{m}{2}\right) \right| \vec{\mu} \right\rangle . \tag{38}$$

Then $\bar{S}_i$ and $\bar{\mathfrak{D}}_i$ see the same final interaction as required by the Faddeev equation [Eq. (8)].

4. Fit of $f(\lambda_0, M) = Re^{i\varphi}$

We have searched for the three kinematical situations considered in Sec. IV B 3: (1) $\theta_1 = 45°$, $\theta_2 = -57°$; (2) $E_1 = 50$ MeV, $\theta_1 = 45°$; (3) $E_1 = 50$ MeV, $\theta_1 = 30°$, and for each point, first the value of R such that $\bar{J}_2$ equals J_2, then the phase φ which allows us to conserve the ratio

$$\bar{J}_{12}/(\bar{J}_1 + \bar{J}_2) = J_{12}/(J_1 + J_2) . \tag{39}$$

The phase is obtained from a second order linear equation which has two solutions φ_+ and φ_- (except when $\bar{J}_1$ differs very much from J_1; case (3) near the FSI peak where no solution has been found). R and $\varphi_\pm$ vary slightly with the kinematics, as shown on Fig. (11) in case (1), but at first approximation one can consider them as constants and extract average values. For example, with

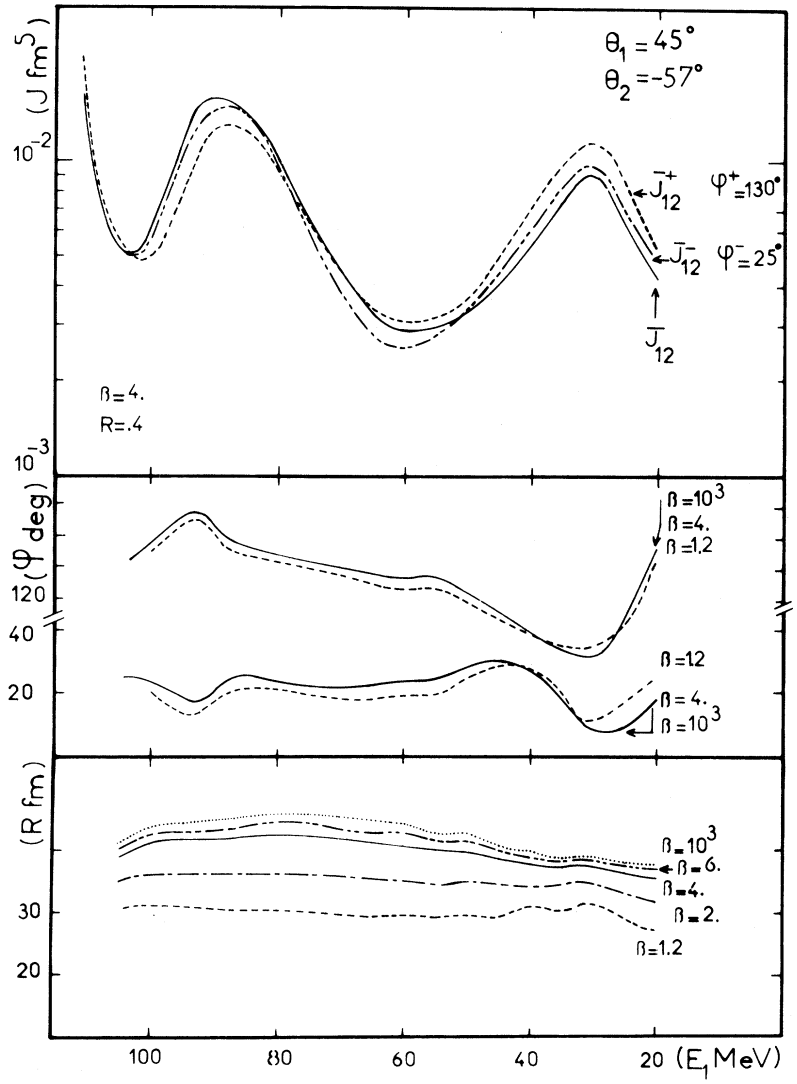

FIG. 11. The lower and central figures show the fitting of the two-body amplitudes $f(\lambda_0, M) = R \exp(i\varphi^{\pm})$ as a function of β in fm^{-1}. The upper figure compares the reference amplitude $\bar{J}_{12}$ [Eq. (39)] with the fitted ones $\bar{J}^{+}_{12}(\beta = 4,\ R = 0.4,\ \varphi^{+} = 130°)$ and $\bar{J}^{-}_{12}(\beta = 4,\ R = 0.4,\ \varphi^{-} = 25°)$.

$\bar{\beta}=4$ fm^{-1}, one obtains

$$\bar{R}=0.40\pm0.02 \text{ fm}, \quad \bar{\varphi}_-=25^\circ\pm5^\circ, \quad \text{and}$$
$$\bar{\varphi}_+=130^\circ\pm10^\circ. \tag{40}$$

For $\beta=6$ fm^{-1}, 1000 fm^{-1}, R is found slightly larger; the phases remain practically unchanged; differences are more important for lower β values.

In conclusion, as we have noticed a good stability for R and φ in spite of very different kinematics, this gives some credibility to our method for fixing $f(\lambda_0, M)$.

The upper part of Fig. (11) analyzes the sensitivity of $\bar{J}_{12}$ to the detailed variations of R and φ by comparing the values $\bar{J}^{\pm}_{12}$ calculated with $\bar{\beta}=4$ fm^{-1}, $\bar{R}=0.4$ fm, $\varphi_-=25^\circ$, or $\varphi_+=130^\circ$ the fitted ones [Eq. (39)]. One sees that the averaging of R and φ changes significantly neither the shape nor the magnitude of this second order contribution. Similar behavior is observed when β is varied.

C. Results and discussion

The FSA cross sections up to second order $\bar{J}^{\pm}_{12}$ and the integral solution $\bar{J}^{\pm}$ corresponding to $\bar{R}=0.4$ fm, $\bar{\varphi}_+=130^\circ$, $\bar{\varphi}_-=25^\circ$, and $\bar{\beta}=4$ fm^{-1} are compared to the experimental data on Fig. 7 for $\theta_1=45^\circ$, $\theta_2=-57^\circ$, on Fig. 8(a) for $E_1=50$ MeV and $\theta_1=45^\circ$, and on Fig. 9(a) for $E_1=50$ MeV and $\theta_1=30^\circ$.

It appears that the multiple scattering process corrects in the expected way the second order contribution. $\bar{J}^+$ best reproduces the experimental shape but overestimates the FSI peak, whereas $\bar{J}^-$ gives a better account of the average magnitude but flattens the structure. The fitting is less satisfactory near the FSI peak in Fig. 9(a). This is mainly due to an overevaluation of $\bar{J}_1$ in this region.

In Figs. 10, 8(a), 8(c), 9(b), and 9(c) partial summations of the multiple scattering up to order 4 have been displayed. They indicate that the expansion has not yet converged for $N=4$.

We have repeated the above calculations for values of R and φ in the range $\bar{R}\pm0.05$ fm and $\bar{\varphi}^{\pm}\pm10^\circ$. This spread is allowed by the fitting procedure of Sec. IV B 4 and corresponds, at the same time, to the range of on-shell variations of the phenomenological two-nucleon potentials used in Sec. III. It appears that the resulting variations are the same order of magnitude for $\bar{J}_{12}$ and $\bar{J}$ and comparable with the flucutations shown in Fig. 5 for realistic potentials up to second order. This might indicate that the sensitivity to the potentials, displayed in the evaluation of J_{12} in Sec. III, could be approximatively preserved but not amplified in an exact calculation.

The two-body off-shell effects in the three-body problem are contained, in our calculations, both in the final N-N wave function $\langle \Delta^{\tau}_{\mu_i} | \vec{\rho} \rangle$ via the half-shell amplitude $t(\vec{\mu}_i, \vec{\chi}_i; \mu_i)$, and in the successive interactions of the multiple scattering expansion. Large off-shell effects (up to 300 MeV) are contained in the final wave function and were analyzed in the second order model. Fixing $\bar{R}$ and $\bar{\varphi}^{\pm}$, parameter β was then varied. One gets very small variations (less than 20%) for β between $\bar{\beta}=4$ fm^{-1} and 1000 fm^{-1}. On the contrary, for $\beta=\beta_0=1.2$ fm^{-1} the ratio $|\bar{J}(\beta_0)-\bar{J}(\bar{\beta})|/\bar{J}(\bar{\beta})$ reaches 200% in some kinematical regions. Let us recall that parameter β determines the off-shell variation of the chosen interaction [Eqs. (26)–(27)] through the form factor $(\beta^2+\lambda^2)/(\beta^2+\lambda_0^2)$ where $\lambda_0=1.82$ fm^{-1} is the on-shell λ value. The sensitivity of the results to an alteration of β is some test of the off-shell intermediate propagation since two-body amplitudes heavily weighted, in the summation, on their on-energy shell point would imply independence of β. The variations observed when β decreases from $\bar{\beta}$ to β_0 indicate that the off-shell values do contribute; but the quasi-invariability of the results for $\beta>\bar{\beta}$ means that intermediate λ are cut to values much less than 4 fm^{-1}. One may conclude that there is, in the intermediate propagations, an effective contribution of the off-shell two-body amplitudes but limited to off-shell deviations $|\lambda-\lambda_0|$ much less than $|4 \text{ fm}^{-1}-\lambda_0|\approx 2$ fm^{-1}.

We noticed that the results for $\bar{R}=0.4$ fm, $\bar{\varphi}^-=25^\circ$, and $\beta=\beta_0=1,2$ fm^{-1} are closer to the experimental values than for $\beta=4$ fm^{-1}. Though this β_0 value does not agree with the off-shell variation of realistic local potentials, which is less pronounced, it might correspond to a better parametrization of an effective isotropic two-nucleon interaction in the three-body problem due to a larger effective range. Let us notice that the inaction with $\bar{R}$, $\bar{\varphi}^-$, and β_0 is similar to the one used by Wallace[22] in an exact three-body calculation. His results at 156 MeV are very similar to ours in comparison to the experimental data as well as for the relative contributions of the multiple scattering expansion. This is indicative of the validity of the fixed scattering center approximation at 156 MeV, though the common deficiency of Wallace calculations and ours is the oversimplified form of the two-body interaction. Thus, when $\bar{J}^{\pm}$ is calculated, instead of $\bar{R}$ and $\bar{\varphi}^{\pm}$, with the fitted values R and $\varphi^{\pm}$, which simulate an angular dependence of the interaction, the agreement with the experimental data is improved.

V. SUMMARY AND CONCLUSION

Experimental data of the $p + {}^2\mathrm{H} \to 2p + n$ reaction at 156 MeV covering the kinematical regions far from the quasifree scattering were analyzed in order to find an answer to the following questions:
(i) Is it possible, through this reaction, to get information on the off-shell two-nucleon t-matrix elements and discriminate among several on-shell equivalent nucleon-nucleon potentials? What is the precision of the calculations required to make a reliable selection?
(ii) What kind of three-body reaction model can give this precision and, more particularly, is it possible to succeed in the framework of a multiple scattering expansion for the three-body amplitude?

In the first part of the present work, the cross sections were calculated up to second order in the Faddeev multiple scattering series, with the input of exact off-shell t-matrix elements corresponding to several phenomenological nucleon-nucleon potentials.

In the kinematical regions of final state interaction where the off-shell effects are the most effective, one gets deviations among the potentials which are larger than the experimental uncertainties. This indicates a potential selectivity of the reaction to the two-nucleon interaction but it appears also that the second order calculations are not precise enough to allow any significant choice.

In the second part, the three-body reaction cross section $\bar{J}$ is evaluated in the framework of a fixed scattering centers approximation which allows an estimation of the complete multiple scattering expansion. We used a simplified two-body interaction, the parameters of which are fitted to reproduce the J_{12} cross section up to second order, calculated in the first part with realistic potentials. The cross section $\bar{J}$ improves the second order calculations in the expected way and gives better agreement with the experimental data.

The two-body interaction implied in our calculations is similar to the one used by Wallace[22] in an exact solution of the Faddeev equation. Our results agree with those of Wallace at 156 MeV, especially with regard to the contributions of the successive multiple scattering terms. This comparison indicates that the FSA model is sensitive enough to validate the following conclusions:
(i) The sensitivity to the nucleon-nucleon potentials would be approximately preserved but not amplified in an exact calculation compared to the second order approximation. This allows us to retain the variations of J_{12} calculated in the first part with several realistic two-nucleon potentials as a test of the sensitivity of the three-body cross section to the potential. Kinematical regions of final state interaction, where the spreading among the potentials is larger than the experimental errors, are particularly suitable for this discrimination. Results of Fig. 5 give also an indication of the required precision of the calculations in order to allow a selection among the potentials.
(ii) At the same time, results of Fig. 5 show that a calculation up to second order terms of the Faddeev expansion is not precise enough for this selection though it describes the qualitative features of the $p + {}^2\mathrm{H} \to 2p + n$ cross sections at 156 MeV.
In the FSA model we found that the expansion has not yet converged in the fourth order. Though the convergence might be different with a realistic two-body interaction including $l > 0$ partial waves, it is probably, in the best case, very slow at 156 MeV. Taking into account the increasing imprecision of the numerical evaluation of successive terms, it is doubtful that one can get enough precision if the Faddeev series is truncated at a small number of terms.

---

†Laboratoire Associé au Centre National de la Recherche Scientifique.

[1]M. Morlet, R. Frascaria, N. Marty, and A. Willis, Nucl. Phys. A191, 385 (1972); M. Morlet, thèse de doctorat d'Etat, Université Paris XI, 1972 (unpublished).
[2]J. P. Didelez, I. D. Goldman, E. Hourany, H. Nakamura, F. Reide, and T. Yuasa, Phys. Rev. C 10, 529 (1974).
[3]L. D. Faddeev, Zh. Eksp. Teor. Fiz. 39, 1459 (1960) [Sov. Phys.—JETP 12, 1014 (1961)].
[4]W. M. Kloet, Ph. D. thesis, University of Utrecht, 1973 (unpublished).
[5]A. F. Kuckes, R. Wilson, and P. F. Cooper, Jr., Ann. Phys. (N.Y.) 15, 193 (1961).
[6]A. H. Cromer, Phys. Rev. 129, 1680 (1963).
[7]A. H. Cromer and E. M. Thorndike, Phys. Rev. 131, 1680 (1963).
[8]C. N. Brown and E. M. Thorndike, Phys. Rev. 177, 2067 (1969).
[9]F. Takeuchi and Y. Sakamoto, Nucl. Phys. A185, 366 (1972).
[10]A. Everett, Phys. Rev. 126, 831 (1962).
[11]M. Morlet, R. Frascaria, N. Marty, and A. Willis, Nucl. Phys. A129, 177 (1969).
[12]M. L'Huillier, Nucl. Phys. A129, 196 (1969).
[13]M. Durand, Nucl. Phys. A201, 312 (1973).
[14]S. Minsmo-Oryu, Prog. Theor. Phys. 45, 386 (1971).
[15]I. E. Carthy and P. C. Tandy, Nucl. Phys. A178, 1 (1971).

[16]D. Gogny, P. Pires, and R. de Tourreil, Phys. Lett. 32B, 591 (1970); and private communications.
[17]R. de Tourreil and D. W. L. Sprung, Nucl. Phys. A201, 193 (1973).
[18]T. Hamada and I. D. Johnston, Nucl. Phys. 34, 382 (1962).
[19]R. V. Reid, Jr., Ann. Phys. (N.Y.) 50, 411 (1968).
[20]J. L. Ballot, M. L'Huillier, and P. Benoist-Gueutal, Phys. Rev. C 12, 725 (1975).
[21]M. L'Huillier, J. L. Ballot, and P. Benoist-Gueutal, in *Proceedings of the International Conference on Nuclear Physics, Munich, 1973*, edited by J. de Boer and H. J. Mang (North-Holland, Amsterdam/American Elsevier, New York, 1973), p. 19.
[22]J. M. Wallace, Phys. Rev. C 8, 1275 (1973).
[23]D. D. Brayshaw, Phys. Rev. D 8, 952 (1973); Phys. Rev. Lett. 32, 382 (1974).
[24]L. L. Foldy and J. D. Walecka, Ann. Phys. (N.Y.) 54, 447 (1969).
[25]E. Kujawski, Ann. Phys. (N.Y.) 74, 567 (1972); Phys. Rev. C 7, 18 (1973).
[26]E. Kujawski and E. Lambert, Ann. Phys. (N.Y.) 81, 591 (1973).
[27]P. Benoist-Gueutal, J. Phys. (Paris) 34, 943 (1973).
[28]M. L'Huillier, thèse de doctorat d'Etat, Université Paris VII, 1974 (unpublished).